AP1S3 Mutations Are Associated with Pustular Psoriasis and Impaired Toll-like Receptor 3 Trafficking

Niovi Setta-Kaffetzi,[1] Michael A. Simpson,[1] Alexander A. Navarini,[1] Varsha M. Patel,[1] Hui-Chun Lu,[2] Michael H. Allen,[1] Michael Duckworth,[1] Hervé Bachelez,[3,4] A. David Burden,[5] Siew-Eng Choon,[6] Christopher E.M. Griffiths,[7] Brian Kirby,[8] Antonios Kolios,[9] Marieke M.B. Seyger,[10] Christa Prins,[11] Asma Smahi,[3] Richard C. Trembath,[1,12] Franca Fraternali,[2] Catherine H. Smith,[1] Jonathan N. Barker,[1,13] and Francesca Capon[1,13,*]

Adaptor protein complex 1 (AP-1) is an evolutionary conserved heterotetramer that promotes vesicular trafficking between the *trans*-Golgi network and the endosomes. The knockout of most murine AP-1 complex subunits is embryonically lethal, so the identification of human disease-associated alleles has the unique potential to deliver insights into gene function. Here, we report two founder mutations (c.11T>G [p.Phe4Cys] and c.97C>T [p.Arg33Trp]) in *AP1S3*, the gene encoding AP-1 complex subunit σ1C, in 15 unrelated individuals with a severe autoinflammatory skin disorder known as pustular psoriasis. Because the variants are predicted to destabilize the 3D structure of the AP-1 complex, we generated *AP1S3*-knockdown cell lines to investigate the consequences of AP-1 deficiency in skin keratinocytes. We found that *AP1S3* silencing disrupted the endosomal translocation of the innate pattern-recognition receptor TLR-3 (Toll-like receptor 3) and resulted in a marked inhibition of downstream signaling. These findings identify pustular psoriasis as an autoinflammatory phenotype caused by defects in vesicular trafficking and demonstrate a requirement of AP-1 for Toll-like receptor homeostasis.

Adaptor protein (AP) complexes are cytosolic heterotetramers that promote the assembly and trafficking of small transport vesicles. Each of the five known complexes (AP-1, AP-2, AP-3, AP-4, and AP-5) is active in a distinct subcellular compartment, where it mediates the delivery of transmembrane proteins to specific target organelles.[1] AP-1 is involved in the transport of cargoes between the *trans*-Golgi network and the endosomes, a process that requires the formation of specialized clathrin-coated vesicles. Similar to other AP complexes, AP-1 consists of two large (γ and β1), one medium (μ1), and one small (σ1) subunit. These are the product of eight genes, which encode multiple isoforms of the β1 (β1A and β1B), μ1 (μ1A and μ1B), and σ1 (σ1A, σ1B, and σ1C) subunits.[2] Of note, the knockout of genes encoding the murine AP-1 γ and μ1A subunits is embryonically lethal.[3] Although this observation underscores the crucial role of AP-1 in cell homeostasis, it also highlights the difficulty of investigating its function in vivo.

The term pustular psoriasis indicates a group of rare and severe inflammatory skin disorders that often manifest with concomitant plaque psoriasis. Generalized pustular psoriasis (GPP [MIM 614204]) is the most severe form of the disease and is characterized by acute, potentially life-threatening episodes of skin pustulation and systemic inflammation. Conversely, palmar plantar pustulosis (PPP) and acrodermatitis continua of Hallopeau (ACH) are chronic, localized, and disabling conditions that affect the palms and soles (PPP) or the tips of the fingers and toes (ACH).[4]

We and others have identified recessive mutations in *IL36RN* (MIM 605507), the gene encoding IL-36 receptor antagonist, in individuals affected by GPP, ACH, and PPP, thus demonstrating a shared genetic basis for acute and chronic forms of pustular psoriasis.[5–7] Importantly, *IL36RN* defects are only found in a minority of affected individuals,[8] an observation that underscores our limited understanding of disease pathogenesis.

Here, we report the identification of pustular psoriasis mutations in *AP1S3* (RefSeq accession number NM_001039569.1), the gene encoding the σ1C subunit of the AP-1 complex.

We undertook the search for disease-causing mutations by means of whole-exome sequencing. To minimize the confounding effects of genetic heterogeneity, we focused on a single disease subtype and examined seven isolated ACH subjects (individuals S0655–S0661 in Table 1; Figure 1A). The study was approved by the research ethics committees of the contributing institutions, and all participants granted their written informed consent. Whole-exome capture was carried out with the Agilent Sure Select

[1]Division of Genetics and Molecular Medicine, King's College London, London SE1 9RT, UK; [2]Randall Division of Cell and Molecular Biophysics, King's College London, London SE1 9RT, UK; [3]Institut National de la Santé et de la Recherche Médicale Unité 781, Institut Imagine, Hopital Necker – Enfant Malades, Paris 75015, France; [4]Department of Dermatology, Sorbonne Paris Cité Université Paris Diderot and Hôpital Saint-Louis, Assistance Publique – Hôpitaux de Paris, Paris 75010, France; [5]Department of Dermatology, University of Glasgow, Glasgow G11 6NT, UK; [6]Department of Dermatology, Hospital Sultanah Aminah, Johor Bahru 80100, Malaysia; [7]Department of Dermatology, University of Manchester, Manchester M6 8HD, UK; [8]Department of Dermatology, St. Vincent University Hospital, Dublin 4, Ireland; [9]Department of Dermatology, Zurich University Hospital, Zurich 8091, Switzerland; [10]Department of Dermatology, Radboud University Nijmegen Medical Centre, 6500HB Nijmegen, the Netherlands; [11]Dermatology Service, Geneva University Hospital, 1211 Geneva 14, Switzerland; [12]Queen Mary University of London, Barts and The London School of Medicine and Dentistry, London EC1M 6QB, UK
[13]These authors contributed equally to this work
*Correspondence: francesca.capon@kcl.ac.uk
http://dx.doi.org/10.1016/j.ajhg.2014.04.005.

Table 1. ACH Subjects Analyzed by Whole-Exome Sequencing

Subject ID	Sex	Origin	Plaque Psoriasis	GPP	Age of Onset (Years)
S0125	female	British	no	yes	10
S0128	female	British	no	yes	45
S0655	female	Polish	yes	no	57
S0656	female	Swiss	yes	no	76
S0657	female	Swiss	no	no	82
S0658	male	Swiss	no	no	49
S0659	female	Irish	no	no	54
S0660	female	Swiss	yes	no	56
S0661	female	British	no	no	39

All subjects were negative for mutations in *IL36RN* and *CARD14*, a locus that has been tentatively implicated in the pathogenesis of GPP.[9] Individuals S0125 and S0128 had been previously exome sequenced by our group.[6]

XT Human All Exome Kit (v.4), and enriched DNA fragments were sequenced on an Illumina HiSeq2000 apparatus. Paired-end reads were aligned to the hg19 reference genome (UCSC Genome Browser) with Novoalign (v.2.07.17, Novocraft Technologies). Over 8.2 Gb of sequence was obtained for each subject, so that >90% of Gencode bases were covered at a depth exceeding 20× (Table S1, available online). Single-nucleotide substitutions and small indels were identified with Samtools (v.0.1.18)[10] and annotated to coding genes with the ANNOVAR package (October 2012 release).[11] The variant profiles thus generated were merged with those of two individuals affected by ACH with concomitant GPP (S0125 and S0128 in Table 1), who were previously exome sequenced by our group.[6] The combined data set was filtered for removal of all synonymous changes and all polymorphisms occurring with >1% frequency in the 1000 Genomes CEU (Utah residents with ancestry from northern and western Europe) data set, the NHLBI Exome Sequencing Project Exome Variant Server, or 1,360 exomes sequenced in house. This identified an average of 485 protein-altering changes per sample (Table S2).

No gene harbored rare homozygous or compound-heterozygous alleles in more than one affected individual. Conversely, 13 loci showed heterozygous changes in four out of nine subjects (Table S3). The use of pathogenicity-prediction software (SIFT[12] and PolyPhen-2[13] for coding alleles and MaxEntScan[14] and Spliceman[15] for splicing variants) indicated that only two genes, *AP1S3* and *MYOM1* (MIM 603508), encompassed variation classified as deleterious

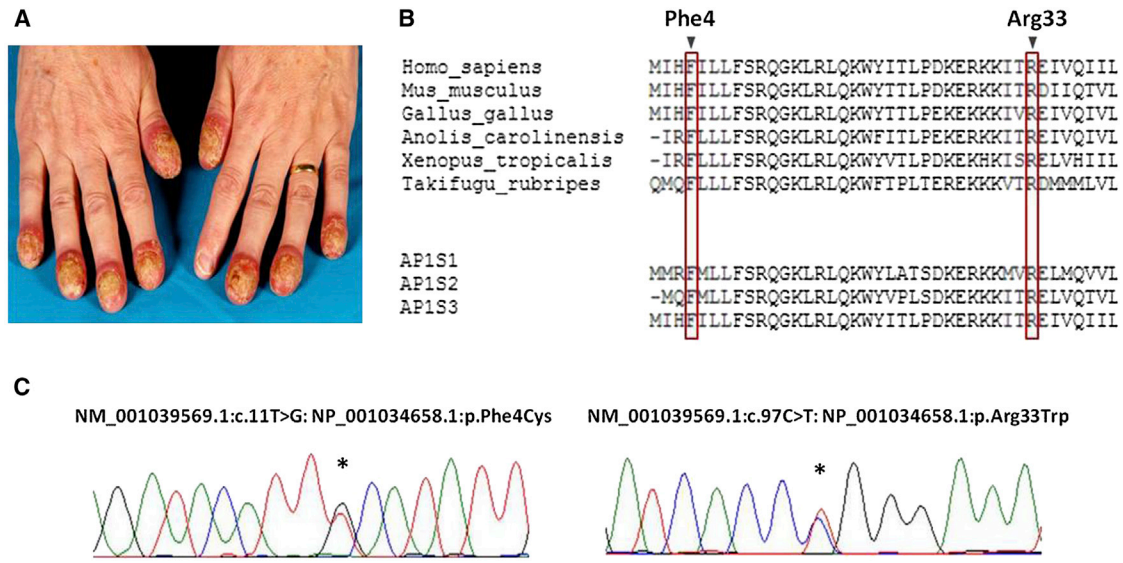

Figure 1. Identification of *AP1S3* Mutations in Individuals Affected by Pustular Psoriasis
(A) Clinical presentation of ACH with active sterile pustules, scaling, nail dystrophy, and digit tapering.
(B) Protein sequence alignments demonstrating the evolutionary conservation of the Phe4 and Arg33 residues.
(C) Representative chromatograms of the c.11T>G (p.Phe4Cys) and c.97C>T (p.Arg33Trp) mutations. The position of the nucleotide change is highlighted by an asterisk.

Table 2. Frequency Distribution of Rare *AP1S3* Variants

	Pathogenicity Prediction						Allele Counts (%)		
Variant (rs ID)	SIFT	PolyPhen-2	PROVEAN	MutationTaster	MutPred	Consensus[a]	Cases	Controls[b]	p Value
c.11T>G (p.Phe4Cys) (rs116107386)	damaging	probably damaging	deleterious	disease causing	damaging	DAMAGING	6/256 (2.3%)	22/3,390 (0.6%)	0.01
c.49C>A (p.Gln17Lys)	tolerated	possibly damaging	deleterious	disease causing	neutral	NEUTRAL	0/256 (0%)	1/3,388 (0.02%)	0.09
c.64A>G (p.Thr22Ala) (rs149183052)	damaging	benign	neutral	disease causing	neutral	NEUTRAL	0/256 (0%)	16/3,322 (0.5%)	0.54
c.95C>T (p.Thr32Ile) (rs78536455)	tolerated	benign	deleterious	polymorphism	neutral	NEUTRAL	1/256 (0.4%)	16/3,388 (0.5%)	0.77
c.97C>T (p.Arg33Trp) (rs138292988)	damaging	probably damaging	deleterious	disease causing	damaging	DAMAGING	9/256 (3.6%)	24/3,388 (0.7%)	2.3×10^{-5}
c.235T>G (p.Leu79Val) (rs34353588)	tolerated	benign	neutral	disease causing	neutral	NEUTRAL	0/256 (0%)	4/3,390 (0.1%)	0.66
c.248T>C (p.Ile83Thr) (rs202157374)	tolerated	benign	deleterious	disease causing	neutral	NEUTRAL	0/256 (0%)	5/3,390 (0.1%)	0.79
Damaging variants[a]							15/256 (5.9%)	46/3,388 (1.4%)	2.5×10^{-7}

[a]Variants were designated as damaging when a high-confidence pathogenicity prediction was returned by at least four out of five programs. All pathogenicity predictions are based on the analysis of *AP1S3* transcript ENST00000396654.
[b]The differences in total allele counts reflect the varying coverage of the relevant nucleotides in the control individuals who were exome sequenced.

by multiple algorithms. Given that the four subjects bearing an *AP1S3* variant all carried the same rare allele (c.97C>T [p.Arg33Trp]), we selected this locus for follow-up. We screened 119 unrelated British individuals (112 with PPP, five with GPP, and two with ACH; Tables S4 and S5) and detected the c.97C>T allele in five additional subjects (four with PPP and one with GPP). Moreover, we identified six subjects (five with PPP and one with GPP) who harbored a c.11T>G (p.Phe4Cys) mutation (Figure 1B and 1C). Thus, *AP1S3* variants were found in all forms of pustular psoriasis but were noticeably enriched among ACH-affected subjects and significantly underrepresented within the PPP data set (Tables S6 and S7).

To further explore the significance of these results, we assessed the frequency and pathogenic potential of the rare *AP1S3* alleles observed in 1,695 unrelated control individuals (Table S8). Although we observed seven coding variants occurring with <1% frequency, we found that c.11T>G and c.97C>T were the only changes predicted to be pathogenic. Importantly, the frequencies of both alleles were significantly higher in pustular psoriasis subjects than in the general population: the c.11T>G mutation appeared in 2.3% of affected individuals, but only 0.6% of control subjects ($p = 0.01$), and c.97C>T appeared in 3.6% of affected individuals, but only 0.7% of control subjects ($p = 2.3 \times 10^{-5}$). The combined analysis of the two mutations yielded $p = 2.5 \times 10^{-7}$ (Table 2), exceeding the threshold for exome-wide significance ($p < 2.5 \times 10^{-6}$).[16]

To investigate whether *AP1S3* mutations were also found in individuals of non-European descent, we analyzed 72 Asian (all with GPP) and four African (two with ACH and two with GPP) subjects. In keeping with the population frequencies documented by the 1000 Genomes Project, we found that none of the above subjects carried the c.11T>G or c.97C>T allele. We observed no other *AP1S3* coding variant, with the exception of a heterozygous c.370C>G (p.Gln124Glu) mutation, found in a single Malay subject and predicted to be benign. Thus, our findings indicate that pustular psoriasis is specifically associated with the c.11T>G and c.97C>T alleles.

We next sought to determine whether the two mutations were the result of a founder effect. Because the late age of disease onset hindered the collection of parental samples, we focused our analysis on the affected subjects, whom we genotyped for a highly polymorphic intragenic (TG) repeat. We found that all c.97C>T subjects were heterozygous for a 214 bp allele, whereas all c.11T>G individuals carried a 218 bp repeat. Given the low population frequency of the 214 and 218 bp alleles, this observation strongly suggests that c.97C>T and c.11T>G are founder mutations and argues against the possibility of de novo inheritance (Table 3). In keeping with these findings, segregation analyses carried out in two representative pedigrees confirmed that the probands (T002206 and T001882, bearing c.11T>G and c.97C>T, respectively) had inherited the disease allele from an unaffected parent. Thus, the lack of family history among subjects with *AP1S3* mutations (Table S6) is likely to reflect the requirement of environmental triggers for disease development. Indeed, it is well recognized that pustular flares are often initiated by infections, pregnancy, or drug exposure.[4]

To explore the consequences of the p.Phe4Cys (c.11T>G) and p.Arg33Trp (c.97C>T) changes, we modeled the structure of AP-1 subunit σ1C (encoded by *AP1S3*) with the Modeler 9 (v.8.0) package.[17] We used the T-Coffee software (v.1.0)[18] to align the sequence of AP-1

Table 3. Association between Intron 1 Repeats and *AP1S3* Mutations

	214 bp Repeat		218 bp Repeat	
	UK Population[a]	c.97C>T Subjects	UK Population[a]	c.11T>G Subjects
Allele counts (frequency)	18/278 (6.5%)	9/18 (50%)	17/278 (6.1%)	6/12 (50%)
Association	$p = 7.0 \times 10^{-9}$		$p = 6.9 \times 10^{-7}$	

[a]A sample of 139 unrelated British individuals genotyped in house.

subunit σ1C with that of the murine AP-1 core[19] (Protein Data Bank ID 1W63), generating 200 models. We selected those with the best Modeler DOPE scores and visualized the p.Phe4Cys and p.Arg33Trp substitutions by using PyMol (v.1.3 Schrödinger). We also modeled the interaction between AP-1 subunit σ1C and its partner μ1A by superimposing human σ1C coordinates on the structure of the murine AP-1 σ1C/μ1A crystal complex.

We found that Phe4 is located within the core of AP-1 subunit σ1C and is part of a cluster of hydrophobic residues, which stabilize the protein and its fold (Figure 2A, top panel). Importantly, the p.Phe4Cys substitution causes the loss of crucial contacts with residues Ile35 and Trp52 and has a likely detrimental effect on the stability of the complex (Figure 2A, bottom panel). We further observed that Arg33 is critically located at the AP-1 σ1C/μ1A interface, where the substitution of a positively charged arginine with a nonpolar tryptophan is likely to disrupt a salt bridge with Glu232 of AP-1 subunit μ1A and substantially weaken the interaction between the two subunits (Figure 2B). In keeping with these predictions, we observed decreased levels of the p.Phe4Cys protein upon transfection of mutant and wild-type (WT) constructs into human embryonic kidney 293 (HEK293) and HaCaT cells. This reduction in AP-1 subunit σ1C accumulation was not observed when a construct encoding the p.Arg33Trp change was transfected, supporting the notion that the p.Phe4Cys substitution specifically disrupts protein stability and folding, whereas p.Arg33Trp is more likely to exert its effect on protein-protein interactions (Figures 2C, 2D, and S1).

Given that AP-1 subunit σ1C is one of the core subunits thought to stabilize AP-1 heterotetramers,[3] we reasoned that p.Phe4Cys and p.Arg33Trp are likely to be loss-of-function changes disrupting the formation of functional AP-1 complexes. Given that the endosomal localization of the innate receptors TLR-7 and TLR-9 is dependent on AP-2 and AP-4,[21] we further hypothesized that AP-1 might be required for the trafficking of the paralog TLR-3 receptor. Thus, we proposed that *AP1S3* deficiency would disrupt TLR-3 translocation to the endosome and result in abnormal downstream signaling.

To explore this hypothesis, we generated two stable *AP1S3*-knockdown cell lines (Figure 3A) through the lentiviral transduction of HaCaT immortalized keratinocytes with targeted small hairpin RNA (shRNA) constructs (Table S9). Because TLR-3 is cleaved by acidic proteases upon reaching the endosomes,[22] we investigated the effects of *AP1S3* silencing by monitoring the levels of full-length and processed receptor. We found that TLR-3 trafficking was disrupted in both knockdown cell lines, where the ratio between endosomal and newly synthesized receptor was markedly reduced. This effect was already noticeable under basal conditions but became more pronounced upon stimulation of TLR-3 with the poly(I:C) ligand (Figure 3B, lanes 2, 4, and 6).

To further explore these findings, we sought to determine whether *AP1S3* deficiency also affects TLR-3-dependent induction of genes encoding type I interferons (IFNs). We stimulated control and knockdown cell lines with poly(I:C) and measured *IFNB1* expression by real-time PCR. In keeping with the results of the previous experiments, we found that the induction of *IFNB1* transcripts was virtually abolished in one knockdown cell line and significantly reduced in the second (Figure 3C).

Having demonstrated that *AP1S3* knockdown disrupts TLR-3 endosomal translocation, we sought to determine whether disease-associated alleles have a similar impact. We reasoned that the p.Phe4Cys change would very likely mimic the effects of gene silencing, given its deleterious impact on protein stability. We therefore focused our attention on the c.97C>T (p.Arg33Trp) mutation. We generated another *AP1S3*-knockdown cell line by silencing gene expression in HEK293 cells (Figure 3D). In keeping with the results obtained in HaCaT keratinocytes, we were able to show that *AP1S3* deficiency resulted in reduced processing of transfected TLR-3 (Figure 3E, left panel). Having validated this experimental system, we investigated the effects of overexpressing WT versus mutant constructs. We found that the transfection of cDNAs encoding the p.Arg33Trp substitution resulted in decreased accumulation of N-ter TLR-3 (Figure 3E, right panel), demonstrating a significant impact on protein function for this disease allele.

The devastating consequences of AP-1 deficiency have been documented in mice[3] and in humans, where recessive truncating mutations in *AP1S1* cause MEDNIK syndrome (mental retardation, enteropathy, deafness, peripheral neuropathy, ichthyosis, and keratodermas [MIM 609313]), a congenital multisystem disorder associated with reduced life expectancy.[23] Thus, the pleiotropic effects of AP-1 deficiency have hindered the identification of specific cellular processes that are controlled by this complex. Although the knockout of genes encoding AP-2

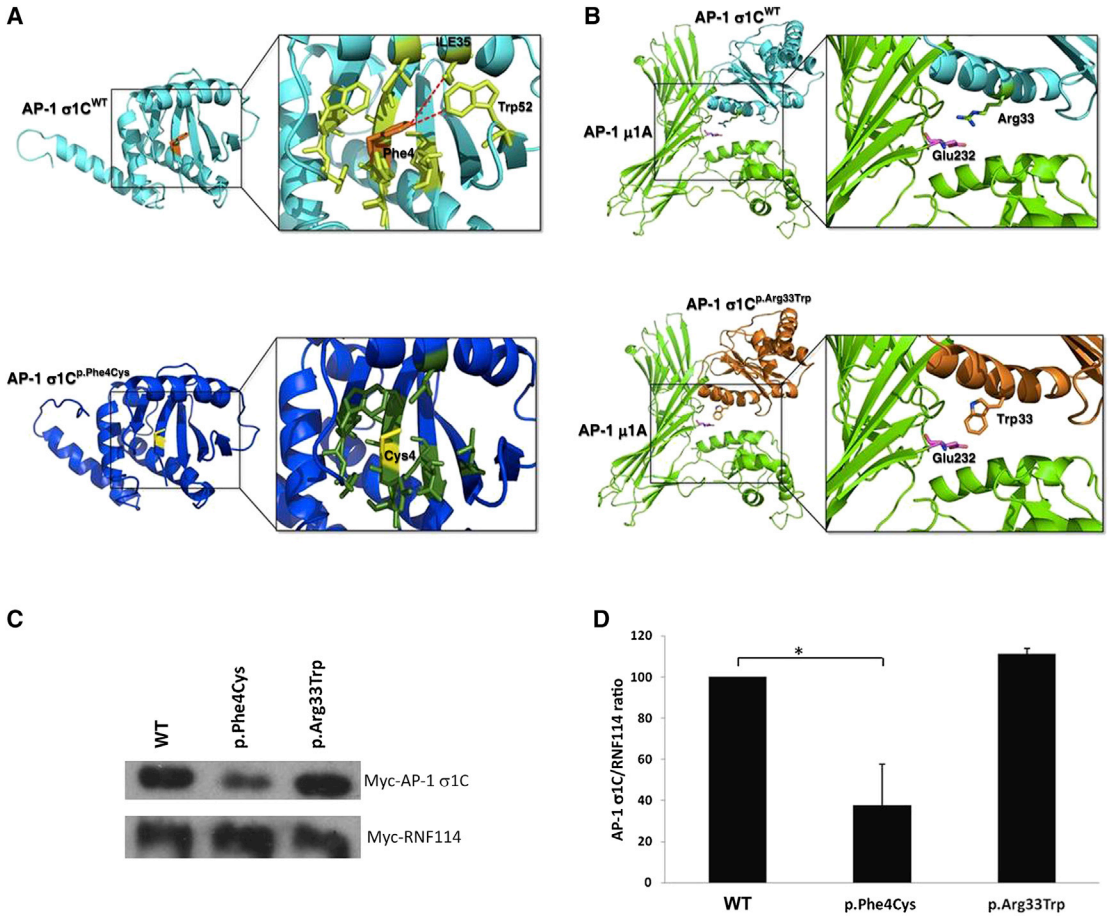

Figure 2. Structural Impact of the p.Phe4Cys and p.Arg33Trp Substitutions
(A) Comparison between WT (AP-1 σ1C^{WT}, cyan) and p.Phe4Cys (AP-1 σ1C$^{p.Phe4Cys}$, blue) proteins. The residues within 6 Å of AP-1 σ1C^{WT} Phe4 and AP-1 σ1C$^{p.Phe4Cys}$ Cys4 are shown in stick representation and are colored in light green and green, respectively. The hydrophobic interactions between Phe4 and its neighboring residues are represented by red dotted lines.
(B) Comparison between WT (AP-1 σ1C^{WT}, cyan) and p.Arg33Trp (AP-1 σ1C$^{p.Arg33Trp}$, orange) proteins. AP-1 σ1C residues Arg33 and Trp33, together with AP-1 σ1A residue Glu232 (which lies within 6 Å of Arg33), are shown in stick representation.
(C) Immunoblot demonstrating the reduced accumulation of p.Phe4Cys proteins. WT and mutant pcDNA3.1-Myc-*AP1S3* constructs were transfected alongside a pcDNA3.1-Myc-*RNF114* plasmid (which was used as a transfection-efficiency and loading control) into HEK293 cells. Protein extracts were analyzed by immunoblot with an anti-Myc antibody (MA1-21316, 1:1,000 dilution, Thermo Scientific). The image is representative of the results obtained in two independent transfections.
(D) Densitometric analysis of the immunoblots described in (C). The ratio between the intensities of the AP-1 σ1C and RNF114 bands was derived with ImageJ.[20] Data are shown as means ± SD of two independent experiments. *$p < 0.05$ (unpaired t test).

subunits is also embryonically lethal,[3] heterozygous missense mutations in *AP2S1* (MIM 602242; encoding AP-2 subunit σ2) have been associated with reduced calcium-sensing receptor endocytosis, which leads to familial hypocalciuric hypercalcemia (MIM 600740).[24] This suggests that the characterization of missense changes in genes encoding AP-1 and AP-2 could help dissect the cellular pathways that are affected by the disruption of each AP complex.

Here, we describe two heterozygous *AP1S3* mutations resulting in severe skin autoinflammation. Our analysis of 128 European and 76 non-European affected individuals has demonstrated that the disease is specifically associated with substitutions in residues Phe4 and Arg33, suggesting a crucial role for these two amino acids. This notion is supported by our structural biology findings and overexpression experiments, which indicate that p.Phe4Cys and p.Arg33Trp are likely to have a detrimental effect on AP-1 function.

To explore the consequences of AP-1 deficiency in skin, we silenced *AP1S3* expression in HaCaT immortalized keratinocytes and HEK293 cells. We found that *AP1S3* knockdown was consistently associated with a significant reduction in TLR-3 trafficking. Moreover, we demonstrated that TLR-3-mediated *IFNB1* induction was markedly decreased in *AP1S3*-knockdown HaCaT keratinocytes. Importantly, IFN-β (the cytokine encoded by *IFNB1*) has well-documented anti-inflammatory functions, as demonstrated by its protective effect in several autoimmune conditions.[25,26] IFN-β also downregulates the production of interleukin-1 (IL-1),[25] the cytokine driving the pathogenesis of most autoinflammatory conditions.[27] Thus,

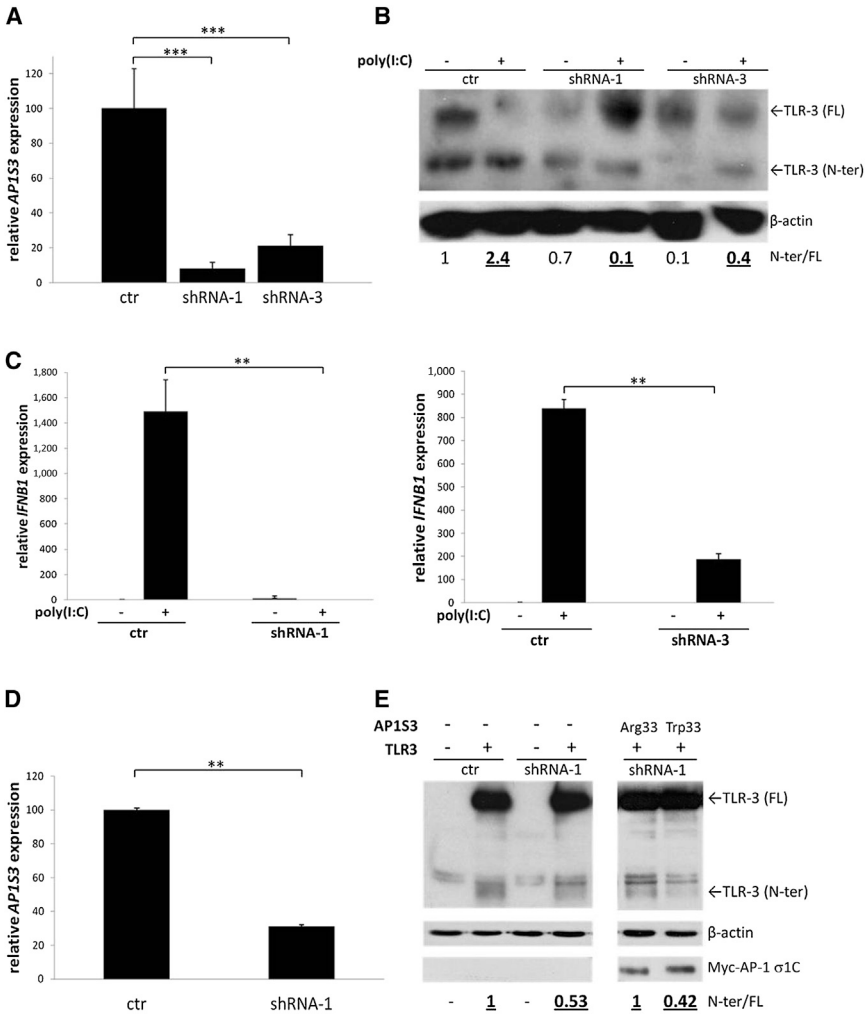

Figure 3. *AP1S3* Deficiency Affects TLR-3 Trafficking and Downstream Signaling

(A) Stable *AP1S3* knockdown in HaCaT immortalized keratinocytes. Approximately 3 × 10^5 HaCaT cells were transduced with the supernatants of HEK293 cultures (5 × 10^5 cells) transfected with 10 μg packaging plasmids (2 μg VSV-G and 8 μg p8.91, Addgene 8454 and 8455) and 2 μg control (ctr; nonsilencing) or silencing shRNA construct. After selection in 10 μg/ml puromycin, the knockdown efficiency was measured by real-time PCR (Table S5) with *PPIA* expression as an internal control (Life Technologies TaqMan assay 4326316E). Data are presented as mean ± SD of two independent RNA extractions. ***$p < 0.001$ (unpaired t test).

(B) *AP1S3* knockdown disrupted trafficking of endogenous TLR-3 in HaCaT keratinocytes. Control and knockdown cells were stimulated with 25 μg/ml poly(I:C) (Invivogen) for 18 hr. The amounts of endosomal (N-ter fragment) and newly synthesized (full-length [FL]) TLR-3 were assessed by immunoblotting with Thermo Fisher Scientific PA5-20184 antibody (1:500 dilution). The intensities of the two bands were measured with ImageJ, and the ratio between the N-ter and FL isoforms was determined for each sample. Bold, underlined font indicates the N-ter/FL ratios observed after poly(I:C) stimulation. β-actin levels determined with Cell Signaling antibody 4970 (1:1,000 dilution) are shown as a loading control.

(C) *AP1S3* knockdown resulted in reduced TLR-3 signaling. Control and knockdown cells were stimulated with 25 μg/ml poly(I:C) for 3 hr, and *IFNB1* induction was measured by real-time PCR (Life Technologies TaqMan assay 4331182) with *PPIA* expression as an internal control. The data are representative of the results obtained in at least two independent experiments and are shown as mean ± SD of two technical duplicates. **$p < 0.01$ (unpaired t test).

(D) Stable *AP1S3* knockdown in HEK293 cells. Approximately 3 × 10^5 cells were transduced with lentiviral shRNA, as described above. The knockdown efficiency was measured by real-time PCR with *PPIA* expression as an internal control. Data are presented as mean ± SD of technical triplicates. **$p < 0.001$ (unpaired t test). The following abbreviation is used: ctr, control cells transduced with a nonsilencing shRNA.

(E) Compared to *AP1S3*-knockdown cells overexpressing WT AP-1 σ1C, *AP1S3*-knockdown cells overexpressing p.Arg33Trp protein showed reduced TLR-3 processing. Left panel: control and knockdown HEK293 cells were transfected with *TLR3* cDNA (Addgene 13084) for 48 hr. The amounts of endosomal (N-ter) and newly synthesized (FL) receptor were assessed by immunoblotting, and the ratio between the two isoforms was determined by densitometry. Right panel: knockdown HEK293 cells were transfected with WT or mutant *AP1S3* cDNA constructs (encoding Arg33 or Trp33, respectively) for 24 hr and with *TLR3* cDNA for a further 48 hr. The amounts of N-ter and FL receptor were monitored by immunoblotting and densitometry. β-actin levels are shown as a loading control. The images are representative of the results obtained from two independent experiments.

our findings raise the intriguing possibility that the reduced IFN response associated with *AP1S3* mutations results in enhanced IL-1 production upon exposure to inflammatory stimuli. Of interest, none of the exome-sequenced subjects lacking *AP1S3* mutations carried any rare variants in other genes encoding AP-1 subunits, indicating that defects in other components of the complex might have distinct phenotypic consequences.

Given the variety of cargoes that are trafficked by the AP-1 complex, alleles associated with pustular psoriasis are likely to affect the localization of additional molecules other than TLR-3. In fact, experiments carried out in HeLa cells have demonstrated that AP-1 depletion causes the deficiency of numerous proteins contributing to epidermal homeostasis (e.g., desmoplakin and clathrin interactor 1) and neutrophil function (e.g., PTPN9 and VPS45).[28] Thus, fully characterizing the impact of *AP1S3* mutations on immune responses will require additional in vitro and ex vivo studies. Given that treatment with IL-1 blockers appears to be beneficial in at least some cases of pustular psoriasis,[29,30] experiments focusing on IL-1 signaling deregulation would be of particular interest because they could deliver important insights into the workings of a druggable disease pathway.

Supplemental Data

Supplemental Data include one figure and nine tables and can be found with this article online at http://dx.doi.org/10.1016/j.ajhg.2014.04.005.

Acknowledgments

We acknowledge support from the Department of Health via the National Institute for Health Research BioResource Clinical Research Facility and comprehensive Biomedical Research Centre award to Guy's and St. Thomas' NHS Foundation Trust in partnership with King's College London and King's College Hospital NHS Foundation Trust. We would like to thank the NHLBI Grand Opportunity (GO) Exome Sequencing Project and its ongoing studies, which provided exome variant calls for comparison: the Lung GO Sequencing Project (HL-102923), the Women's Health Initiative Sequencing Project (HL-102924), the Broad GO Sequencing Project (HL-102925), the Seattle GO Sequencing Project (HL-102926), and the Heart GO Sequencing Project (HL-103010). This work was supported by the National Psoriasis Foundation through a discovery grant to F.C. The exome data for British healthy control individuals were provided by TwinsUK, which is funded by grants from the Wellcome Trust and the European Commission Seventh Framework Programme (FP7/2007-2013). N.S.K.'s PhD studentship is funded by the British Skin Foundation (grant 3007s). A.A.N. is supported by Swiss National Science Foundation grant PASMP3_140074/WGS.

Received: December 19, 2013
Accepted: April 9, 2014
Published: May 1, 2014

Web Resources

The URLs for data presented herein are as follows:

1000 Genomes, http://browser.1000genomes.org
Addgene, https://addgene.org
ImageJ, http://imagej.nih.gov/ij/
MaxEntScan::score3ss, http://genes.mit.edu/burgelab/maxent/Xmaxentscan_scoreseq_acc.html
MutationTaster, http://www.mutationtaster.org/
MutPred, http://mutpred.mutdb.org/
NHLBI Exome Sequencing Project (ESP) Exome Variant Server, http://evs.gs.washington.edu/EVS/
Online Mendelian Inheritance in Man (OMIM), http://www.omim.org/
PolyPhen-2, http://genetics.bwh.harvard.edu/pph2/
Protein Data Bank in Europe (PDBe), http://www.ebi.ac.uk/pdbe/
PROVEAN, http://provean.jcvi.org/index.php
SIFT, http://sift.jcvi.org/
Spliceman, http://fairbrother.biomed.brown.edu/spliceman/

References

1. Hirst, J., Barlow, L.D., Francisco, G.C., Sahlender, D.A., Seaman, M.N., Dacks, J.B., and Robinson, M.S. (2011). The fifth adaptor protein complex. PLoS Biol. *9*, e1001170.
2. Ren, X., Farías, G.G., Canagarajah, B.J., Bonifacino, J.S., and Hurley, J.H. (2013). Structural basis for recruitment and activation of the AP-1 clathrin adaptor complex by Arf1. Cell *152*, 755–767.
3. Robinson, M.S. (2004). Adaptable adaptors for coated vesicles. Trends Cell Biol. *14*, 167–174.
4. Griffiths, C.E.M., and Barker, J.N. (2010). Psoriasis. In Rook's Textbook of Dermatology, T. Burns, S. Breathnach, N. Cox, and C. Griffiths, eds. (Chichester: Wiley-Blackwell), 20.21–20.60.
5. Marrakchi, S., Guigue, P., Renshaw, B.R., Puel, A., Pei, X.Y., Fraitag, S., Zribi, J., Bal, E., Cluzeau, C., Chrabieh, M., et al. (2011). Interleukin-36-receptor antagonist deficiency and generalized pustular psoriasis. N. Engl. J. Med. *365*, 620–628.
6. Onoufriadis, A., Simpson, M.A., Pink, A.E., Di Meglio, P., Smith, C.H., Pullabhatla, V., Knight, J., Spain, S.L., Nestle, F.O., Burden, A.D., et al. (2011). Mutations in IL36RN/IL1F5 are associated with the severe episodic inflammatory skin disease known as generalized pustular psoriasis. Am. J. Hum. Genet. *89*, 432–437.
7. Setta-Kaffetzi, N., Navarini, A.A., Patel, V.M., Pullabhatla, V., Pink, A.E., Choon, S.E., Allen, M.A., Burden, A.D., Griffiths, C.E., Seyger, M.M., et al. (2013). Rare pathogenic variants in IL36RN underlie a spectrum of psoriasis-associated pustular phenotypes. J. Invest. Dermatol. *133*, 1366–1369.
8. Capon, F. (2013). IL36RN mutations in generalized pustular psoriasis: just the tip of the iceberg? J. Invest. Dermatol. *133*, 2503–2504.
9. Jordan, C.T., Cao, L., Roberson, E.D., Pierson, K.C., Yang, C.F., Joyce, C.E., Ryan, C., Duan, S., Helms, C.A., Liu, Y., et al. (2012). PSORS2 is due to mutations in CARD14. Am. J. Hum. Genet. *90*, 784–795.
10. Li, H., Handsaker, B., Wysoker, A., Fennell, T., Ruan, J., Homer, N., Marth, G., Abecasis, G., and Durbin, R.; 1000 Genome Project Data Processing Subgroup (2009). The Sequence Alignment/Map format and SAMtools. Bioinformatics *25*, 2078–2079.
11. Wang, K., Li, M., and Hakonarson, H. (2010). ANNOVAR: functional annotation of genetic variants from high-throughput sequencing data. Nucleic Acids Res. *38*, e164.
12. Kumar, P., Henikoff, S., and Ng, P.C. (2009). Predicting the effects of coding non-synonymous variants on protein function using the SIFT algorithm. Nat. Protoc. *4*, 1073–1081.
13. Adzhubei, I., Jordan, D.M., and Sunyaev, S.R. (2013). Predicting functional effect of human missense mutations using PolyPhen-2. Curr. Protoc. Hum. Genet. *Chapter 7*, 20.
14. Yeo, G., and Burge, C.B. (2004). Maximum entropy modeling of short sequence motifs with applications to RNA splicing signals. J. Comput. Biol. *11*, 377–394.
15. Lim, K.H., and Fairbrother, W.G. (2012). Spliceman—a computational web server that predicts sequence variations in pre-mRNA splicing. Bioinformatics *28*, 1031–1032.
16. Kiezun, A., Garimella, K., Do, R., Stitziel, N.O., Neale, B.M., McLaren, P.J., Gupta, N., Sklar, P., Sullivan, P.F., Moran, J.L., et al. (2012). Exome sequencing and the genetic basis of complex traits. Nat. Genet. *44*, 623–630.
17. Eswar, N., Eramian, D., Webb, B., Shen, M.Y., and Sali, A. (2008). Protein structure modeling with MODELLER. Methods Mol. Biol. *426*, 145–159.
18. Notredame, C., Higgins, D.G., and Heringa, J. (2000). T-Coffee: A novel method for fast and accurate multiple sequence alignment. J. Mol. Biol. *302*, 205–217.
19. Heldwein, E.E., Macia, E., Wang, J., Yin, H.L., Kirchhausen, T., and Harrison, S.C. (2004). Crystal structure of the clathrin adaptor protein 1 core. Proc. Natl. Acad. Sci. USA *101*, 14108–14113.

20. Schneider, C.A., Rasband, W.S., and Eliceiri, K.W. (2012). NIH Image to ImageJ: 25 years of image analysis. Nat. Methods *9*, 671–675.
21. Lee, B.L., Moon, J.E., Shu, J.H., Yuan, L., Newman, Z.R., Schekman, R., and Barton, G.M. (2013). UNC93B1 mediates differential trafficking of endosomal TLRs. Elife *2*, e00291.
22. Garcia-Cattaneo, A., Gobert, F.X., Müller, M., Toscano, F., Flores, M., Lescure, A., Del Nery, E., and Benaroch, P. (2012). Cleavage of Toll-like receptor 3 by cathepsins B and H is essential for signaling. Proc. Natl. Acad. Sci. USA *109*, 9053–9058.
23. Montpetit, A., Côté, S., Brustein, E., Drouin, C.A., Lapointe, L., Boudreau, M., Meloche, C., Drouin, R., Hudson, T.J., Drapeau, P., and Cossette, P. (2008). Disruption of AP1S1, causing a novel neurocutaneous syndrome, perturbs development of the skin and spinal cord. PLoS Genet. *4*, e1000296.
24. Nesbit, M.A., Hannan, F.M., Howles, S.A., Reed, A.A., Cranston, T., Thakker, C.E., Gregory, L., Rimmer, A.J., Rust, N., Graham, U., et al. (2013). Mutations in AP2S1 cause familial hypocalciuric hypercalcemia type 3. Nat. Genet. *45*, 93–97.
25. González-Navajas, J.M., Lee, J., David, M., and Raz, E. (2012). Immunomodulatory functions of type I interferons. Nat. Rev. Immunol. *12*, 125–135.
26. Wang, Y., Shaked, I., Stanford, S.M., Zhou, W., Curtsinger, J.M., Mikulski, Z., Shaheen, Z.R., Cheng, G., Sawatzke, K., Campbell, A.M., et al. (2013). The autoimmunity-associated gene PTPN22 potentiates toll-like receptor-driven, type 1 interferon-dependent immunity. Immunity *39*, 111–122.
27. Aksentijevich, I., and Kastner, D.L. (2011). Genetics of monogenic autoinflammatory diseases: past successes, future challenges. Nat. Rev. Rheumatol. *7*, 469–478.
28. Hirst, J., Borner, G.H., Antrobus, R., Peden, A.A., Hodson, N.A., Sahlender, D.A., and Robinson, M.S. (2012). Distinct and overlapping roles for AP-1 and GGAs revealed by the "knocksideways" system. Curr. Biol. *22*, 1711–1716.
29. Hüffmeier, U., Wätzold, M., Mohr, J., Schön, M.P., and Mössner, R. (2014). Successful therapy with anakinra in a patient with generalized pustular psoriasis carrying IL36RN mutations. Br. J. Dermatol. *170*, 202–204.
30. Rossi-Semerano, L., Piram, M., Chiaverini, C., De Ricaud, D., Smahi, A., and Koné-Paut, I. (2013). First clinical description of an infant with interleukin-36-receptor antagonist deficiency successfully treated with anakinra. Pediatrics *132*, e1043–e1047.